Compact binary merger rates from LIGO-Virgo's first and second observing runs

Shasvath J. Kapadia
CSGC-2020

INTERNATIONAL CENTRE *for* THEORETICAL SCIENCES
TATA INSTITUTE OF FUNDAMENTAL RESEARCH

LSC LIGO Scientific Collaboration
VIRGO

LVC catalog paper (GWTC-1), arXiv 1709.02421 (2018), LIGO Document G1802354

Overview

An Important Astrophysical Question

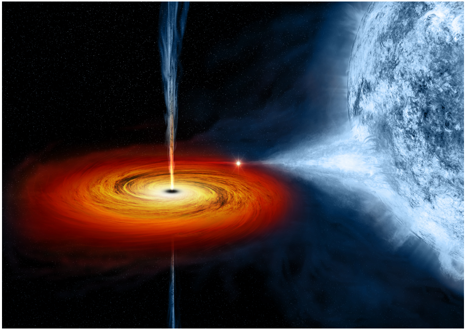

Image: NASA (2012)

- Stellar mass binary models
- Formation Channels for Compact Binaries
- **Which, if any, are preferred by Nature ?**

Motivation for Rate Estimation

- Physical processes uncertain
- Rates of mergers predicted sensitive to assumptions

- **Observed rates can help constrain uncertainties, and identify Nature's preferred model(s)**

Gravitational Waves (GWs)

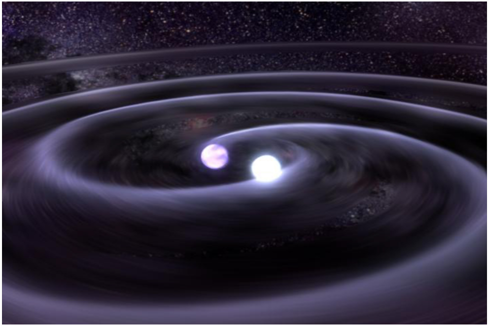

Figure: Coalescing Compact Binaries (CBCs) radiate GWs.

- Perturbation in spacetime metric:

$$g_{\alpha\beta} = \eta_{\alpha\beta} \text{ (Flat Spacetime)} + h_{\alpha\beta} \text{ (GW)} \quad (1)$$

- Produced by time-varying mass-quadrupole moments.

Rates from GWs

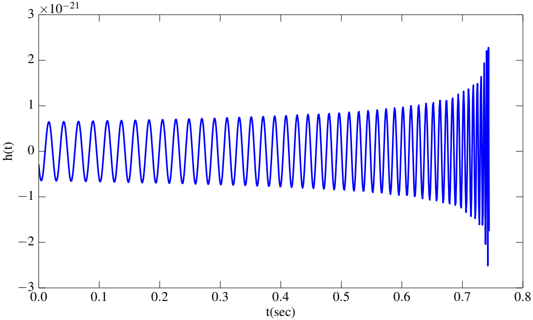

Figure: GW signals encode information about CBCs that produce them: **masses, spins, tides, ...**

- **Detect GWs ⇒ masses ⇒ estimate rates of CBCs**

The LIGO-Virgo Network of Ground-Based Detectors

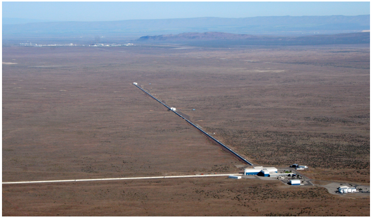

(a) LIGO Hanford

(b) LIGO Livingston

(c) Virgo (Italy)

Images: LIGO Caltech

Detecting GWs since 2015 ...

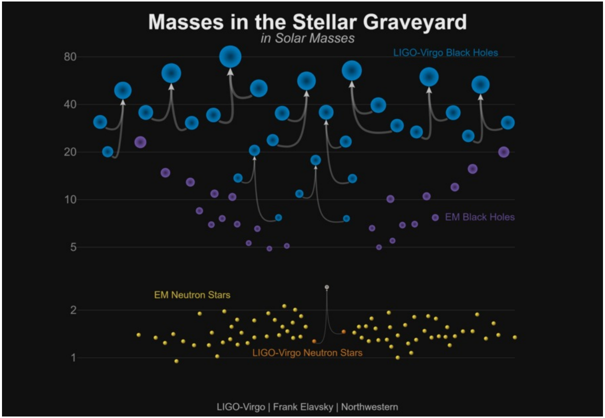

Image: ligo.org

Figure: The LIGO-Virgo network has detected 10 BBHs and 1 BNS over the course of two observing runs: O1 and O2

Detection Method: Matched Filtering

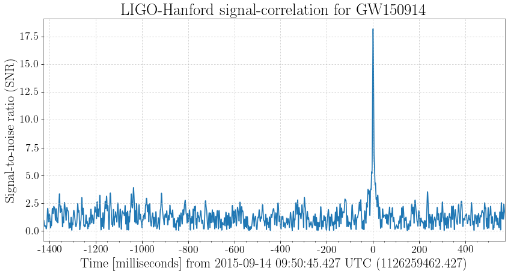

Figure: SNR: $\rho^2 \equiv (s|\hat{h})$, $() \equiv$ Noise-weighted inner product

- Detector Data: $s(t)$ [Strain] $= n(t)$ [Noise] $+ h(t)$ [GW]
- Matched Filtering optimal for stationary Gaussian noise

Two Drawbacks of Matched Filtering

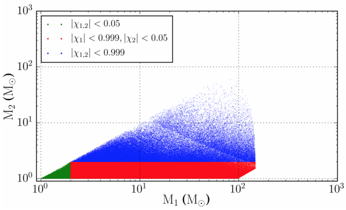

(a) Template bank in component mass space.

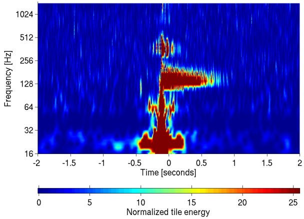

(b) Example of a high SNR "glitch" event

1. Which template to use? – Use bank of templates, determine optimal template
2. Real noise can be non-stationary and non-Gaussian – Construct enhancements to SNR

Detection Pipelines

Figure: Data analysis pipelines used for the estimation of CBC rates

- Elaborate softwares to run filtering jobs efficiently
- **Different** ranking statistics per pipeline
- This talk will focus on GstLAL– based results
- Ranking statistic L
- Complicated function of SNR, as well as other params

Foreground and Background Models

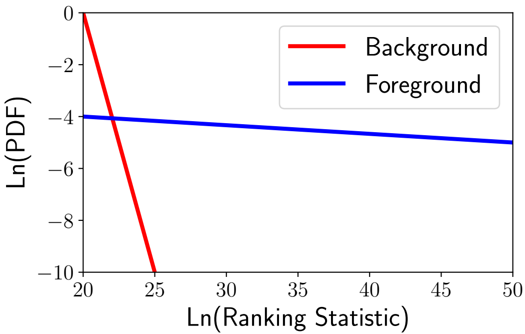

- $b(L) \equiv p(L \mid \text{noise})$ – background model from real data
- $f(L) \equiv p(L \mid \text{signal})$ – foreground model from simulated data
- $f(L)$ is **Universal**

Trigger Significance

- How likely is it that a candidate event with ranking statistic L was triggered by a GW ?

1. **Bayes Factor:** $k(L) \equiv \frac{f(L)}{b(L)}$
2. **False-Alarm-Rate** from $b(L)$ PDF

Poisson counts

Assumption: Triggers produced by astrophysical GWs (f), or terrestrial phenomena (b), occur as independent **Poisson processes**

1. $P(n \mid \Lambda) = \frac{\Lambda^n}{n!} \exp(-\Lambda)$
2. $n \equiv$ number of events of type (f) or (b).
3. $\Lambda \equiv$ Poisson mean for events of type (f) or (b)

Rates from Poisson counts

- $\langle VT \rangle \equiv$ average **spacetime volume sensitivity** of the detector to astrophysical signals
- **Astrophysical Rate**: $R = \frac{\Lambda_f}{\langle VT \rangle}$

Primary Task:

Determine a **posterior** conditional PDF on the **Astrophysical Poisson mean** for the experiment: $p(\Lambda_f|\vec{x})$,

where: $\vec{x} \equiv \{x_1, x_2, \ldots, x_N\}$ is the data set consisting of triggers above some predefined ranking-statistic threshold produced during the experiment.

Previously, in O1

- n confident detections
- Assume *perfect* classification of triggers
- Likelihood on Λ_f:
  - Poisson distributed for n events
  - $p(\vec{x}|\Lambda_f) = p(n \mid \Lambda_f)$
- Choose prior, use Bayes theorem to acquire posterior

Example: Zero confident BNS detections in O1, so $p(\vec{x}|\Lambda_{\mathrm{BNS}}) = \exp(-\Lambda_{\mathrm{BNS}})$. Thus:

$$p(\Lambda_{\mathrm{BNS}}|\vec{x}) \propto p(\Lambda_{\mathrm{BNS}}) \exp(-\Lambda_{\mathrm{BNS}}) \tag{2}$$

Problems with this method

- Triggers can only be classified with a finite FAR
- O1: BNS rates set a threshold of FAR <= 1/100yrs
- Two concerns:
  1. Noise trigger ⇒ FAR <= 1/100yrs
  2. Astrophysical triggers ⇒ FAR > 1/100yrs
- **Need a threshold-independent method**

The FGMC Posterior [1]

$$p(\Lambda_f, \Lambda_b|\vec{x}) \propto p(\Lambda_f, \Lambda_b) e^{-\Lambda_f - \Lambda_b} \prod_{j=1}^{N} [\Lambda_b + k(L_j)\Lambda_f] \tag{3}$$

- Bayes Factor: $k(L_j) \equiv \frac{f(L_j)}{b(L_j)}$
- Key Features:
  1. No need to pre-select highly significant events
  2. Bayes Factors evaluate significance

[1] Farr, Gair, Mandel, Cutler (2015), arXiv:1302.5341

Targeted CBC rates [2]:

- Events from multiple classes ?
- Example: O2-run had BBH events and a BNS event
- Need joint posterior on Poisson means for distinct astrophysical classes:

$$\vec{\Lambda}_f \equiv \{\Lambda_{\mathrm{BNS}}, \Lambda_{\mathrm{BBH}}, \ldots\} \quad (4)$$

- Multi-component posterior:

$$p(\vec{\Lambda}_f, \Lambda_b|\vec{x}) \propto p(\vec{\Lambda}_f, \Lambda_b) e^{-\vec{\Lambda}_f\cdot\vec{u}-\Lambda_b} \prod_{j=1}^{N} \left[\Lambda_b + \vec{k}(x_j)\cdot\vec{\Lambda}_f\right] \quad (5)$$

- Bayes Factor: $\vec{k}(x_j) \equiv \frac{1}{b(L_j)}\{f_{\mathrm{BNS}}(x_j), f_{\mathrm{BBH}}(x_j), \ldots\}$

[2] Kapadia et al (2019), arXiv:1903.06881

Source-specific Signal Models:

- Redistribute $f(L)$ across astrophysical classes with template weights:

$$f_\alpha(x) = f(L) \times w_\alpha(m), \qquad \alpha = \mathrm{BNS}, \mathrm{BBH}, \ldots \tag{6}$$

- m $\equiv$ template parameter(s) (could be masses, spins)
- w_α accounts for how signals from astrophysical source α distribute themselves in the template bank:
  1. Template params $\neq$ Source params
  2. Add simulated α-signals to data and recover

Estimating template weights

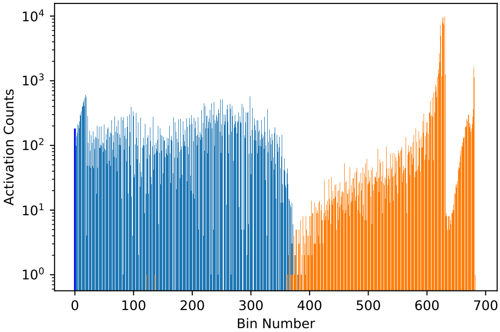

Figure: GstLAL divides the template bank into bins, in the space of intrinsic parameters (masses and spins). Distinct portions of the template bank get activated when recovering BNS (BLUE) and BBH (ORANGE) signals. w_α determined by relative frequency of activation.

Marginalized Poisson Counts Posteriors

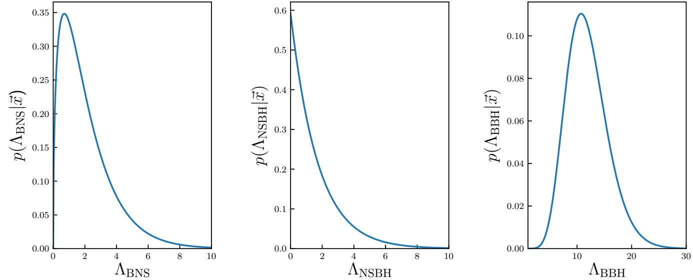

Figure: A joint FGMC posterior on $\Lambda_{\rm BNS}, \Lambda_{\rm NSBH}, \Lambda_{\rm BBH}, \Lambda_b$ was constructed using O1-O2 triggers with $\ln L > 14$. Marginalized posteriors for each of the astrophysical categories are plotted above

Spacetime Volume Integral [3]

$$\langle VT\rangle_{\{\theta\}} = T_{\mathrm{obs}} \int_0^\infty f(z|\{\theta\}) \frac{dV}{dz} \frac{1}{1+z} dz.$$

- $\langle VT\rangle_{\{\theta\}}$: **Estimate of Spacetime Volume Visible to Detectors**
- T_{obs}: **Detector Frame Observation Time**
- $f(z|\{\theta\})$: **Fraction of Differential Volume Accessible to the detector**
- $\frac{dV}{dz}$: **Differential Volume**
- $\frac{1}{1+z}$: **Source Frame Time to Detector Frame Time Conversion Factor**

[3] LVC Catalog Paper (GWTC-1) (2018), arXiv:1811.12907

Spacetime Volume Sensitivities

- Counts → Rates: $R_\alpha = \frac{\Lambda_\alpha}{\langle VT \rangle_\alpha}$
- Method:
  1. Inject signals of class α, with an assumed distribution
  2. Uniform in comoving volume
  3. Recover signals with pipeline
  4. $\langle VT \rangle_\alpha = \frac{N_{\rm rec}}{N_{\rm inj}} \langle VT \rangle_{\rm inj}$
  5. **Important Caveat:** $\langle VT \rangle_\alpha$ estimation is sensitive to the injected distribution

Rates from O1-O2 data:

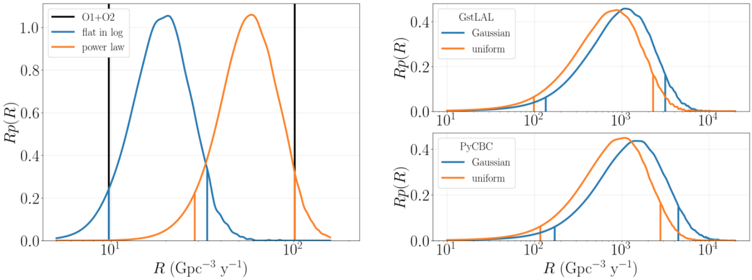

Figure: Binary Black Hole (left) and Binary Neutron Star (right) merger rate posteriors PDFs.[4] At 90% confidence BBH: $9.7 - 101\ \text{Gpc}^{-3}\text{yr}^{-1}$, BNS: $110 - 3840\ \text{Gpc}^{-3}\text{yr}^{-1}$

[4] LVC Catalog Paper (GWTC-1) (2018), arXiv:1811.12907

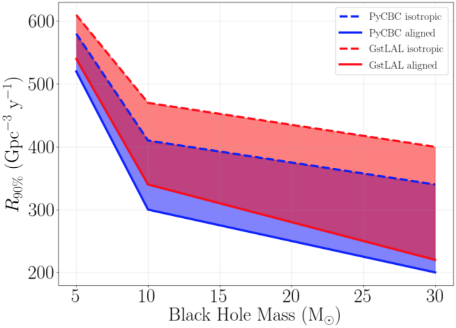

Figure: Neutron Star-Black Hole binary rate upper limits at 90% confidence.[5]

Max value: $610\ \mathrm{Gpc}^{-3}\mathrm{yr}^{-1}$

[5] LVC Catalog Paper (GWTC-1) (2018), arXiv:1811.12907

Summary and Outlook

- Threshold-independent rate-evaluation
- Joint rate-estimates for CBC categories
- Use of mass-based template weighting
- Method not limited to mass-based re-weighting
- E.g: Redshift-dependent re-weighting + rates [6]

[6] E. Chase et al (in preparation)

Source-Specific Probabilities of Astrophysical Origin [7]:

- Probability that event x_j belongs to astrophysical class α:

$$P_\alpha(x_j|\vec{\Lambda}_f, \Lambda_b) = \frac{k_\alpha(x_j)\Lambda_\alpha}{\Lambda_b + \vec{k}(x_j)\cdot\vec{\Lambda}_f} \tag{7}$$

- $\vec{\Lambda}_f, \Lambda_b$ are not known exactly
- Marginalize w.r.t posterior on Poisson means:

$$P_\alpha(x_j|\vec{x}) = \frac{k_\alpha(x_j)\langle\Lambda_\alpha\rangle}{\langle\Lambda_b\rangle + \vec{k}(x_j)\cdot\langle\vec{\Lambda}_f\rangle} \tag{8}$$

[7] Kapadia et al (2019), arXiv:1903.06881

Table of Astrophysical Probabilities for O1-O2 triggers [8]

	GstLAL				
	terrestrial	BNS	NSBH	BBH	astrophysical
GW150914	0	0	0.0064	0.99	1
151008 [a]	–	–	–	–	–
151012A	0.98	0.022	0.0012	0	0.023
GW151012	0.001	0	0.031	0.97	1
151116 [b]	–	–	–	–	–
GW151226	0	0	0.12	0.88	1
161202	0.97	0.034	0	0	0.034
161217	0.98	0	0.011	0.0078	0.018
GW170104	0	0	0.0028	1	1
170208	0.98	0	0.011	0.0088	0.02
170219	0.98	0.019	0	0	0.02
170405	1	0.004	0	0	0.004
170412	0.94	0	0.029	0.032	0.06
170423	0.91	0.086	0	0	0.086
GW170608	0	0	0.084	0.92	1
170616 [b]	–	–	–	–	–
170630	0.98	0.02	0	0	0.02
170705	0.99	0	0.006	0.0061	0.012
170720	0.99	0	0.0077	0.002	0.0097
GW170729	0.018	0	0	0.98	0.98
GW170809	0	0	0.0064	0.99	1
GW170814	0	0	0.0024	1	1
GW170817	0	1	0	0	1
GW170818	0	0	0.0053	0.99	1
GW170823	0	0	0.0059	0.99	1

[8] LVC Catalog Paper (GWTC-1) (2018), arXiv:1811.12907

Astrophysical Probabilities in Low-Latency

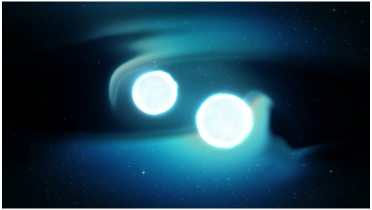

(a) BNS merger

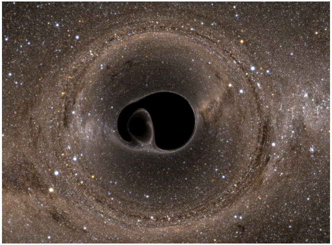

(b) BBH merger

Figure: Low-Latency determination and reporting of astrophysical probabilities useful for astronomers to make follow-up decisions

Testing the extended FGMC method

- Simulated signals added to O1-O2 noise
- 100 BBHs
- 30 BNSs
- 10,10,10 NSBHs with BHs = 5, 10, 30 $M_\odot$

Counting and Confusion